Designed Nanostructured Pt Film for Electrocatalytic Activities by Underpotential Deposition Combined Chemical Replacement Techniques

Minghua Huang, Yongdong Jin, Heqing Jiang, Xuping Sun, Hongjun Chen, Baifeng Liu, Erkang Wang, and Shaojun Dong*

State Key Laboratory of Electroanalytical Chemistry, Changchun Institute of Applied Chemistry, Chinese Academy of Sciences, Changchun, Jilin, 130022, People's Republic of China, and Graduate School of Chinese Academy of Sciences, Beijing, 100039, People's Republic of China

Received: March 30, 2005; In Final Form: June 27, 2005

Multiple-deposited Pt overlayer modified Pt nanoparticle (MD-Pt overlayer/PtNPs) films were deliberately constructed on glassy carbon electrodes through alternately multiple underpotential deposition (UPD) of Ag followed redox replacement reaction by Pt (II) cations. The linear and regular growth of the films characterized by cyclic voltammetry was observed. Atomic force spectroscopy (AFM) provides the surface morphology of the nanostructured Pt films. Rotating disk electrode (RDE) voltammetry and rotating ring-disk electrode (RRDE) voltammetry demonstrate that the MD-Pt overlayer/PtNPs films can catalyze an almost four-electron reduction of O_2 to H_2O in air-saturated 0.1 M H_2SO_4. Thus-prepared Pt films behave as novel nanostructured electrocatalysts for dioxygen reduction and hydrogen evolution reaction (HER) with enhanced electrocatalytic activities, in terms of both reduction peak potential and peak current, when compared to that of the bulk polycrystalline Pt electrode. Additionally, it is noted that after multiple replacement cycles, the electrocatalytic activities improved remarkably, although the increased amount of Pt is very low in comparison to that of pre-modified PtNPs due to the intrinsic feature of the UPD-redox replacement technique. In other words, the electrocatalytic activities could be improved markedly without using very much Pt by the technique of tailoring the catalytic surface. These features may provide an interesting way to produce Pt catalysts with a reliable catalytic performance as well as a reduction in cost.

Introduction

Electrocatalytic reactions play a vital role in emerging technologies related to environmental and energy-related applications, such as fuel cells that are energy sources in an attempt to relieve the pollution and energy crisis. In many electrochemical reactions, the hydrogen evolution reaction occurring in acid media ($H^+ + e^- \rightarrow 1/2H_2$) and the four-electron electroreduction of dioxygen to water ($O_2 + 4H^+ + 4e^- \rightarrow 2H_2O$) is extensively investigated. The former is of considerable significance in hydrogen−oxygen fuel cells, hydrogen embrittlement, electrodeposition of metals in acid media, and so on.[1,2] The latter is the cathode reaction of most fuel cells that utilize dioxygen as the reducible reactant.[3−5] The fact that the electroreduction of dioxygen requires high current density, low overpotential, and nearly synchronous delivery of four electrons gave rise to many innovative electrocatalyst designs.[6] Among various alternative candidates, platinum (Pt) and Pt-based materials are still the indispensable and most effective electrocatalysts employed. However, the high cost and limited supply of Pt constitute a barrier of the commercialization of fuel cells. Therefore, it is necessary to design economical and effective Pt-based catalysts with low loading from the viewpoint of practical applications.

At the same time, the rapid development of nanoscience in recent years opens a way of designing highly efficient catalysts with large surface-to-volume ratios from the controlled nanoscale structures, along with huge savings in the fabrication costs.[7−9] Many efforts have focused on the development of techniques to produce Pt catalysts with a high surface area to achieve reliable catalytic performance and to utilize efficiency.[10] For example, various nanosized Pt-alloy electrocatalysts with narrow size distribution[11,12] and nanocomposite multilayer films containing Pt nanoparticles[13,14] were exploited to study the electrocatalytic activities for dixogen reduction. In addition, Pt hollow nanospheres[7] and thin mesoporous Pt films[15] were also deliberately designed recently and exhibited enhanced electrocatalytic performance with a cost reduction.

Since surface-catalyzed reactions are extremely sensitive to the details of the catalytic surface,[16] the deliberate tailoring of the catalyst surface is an interesting target for the improvement of the catalytic performance. Recently, a new metal deposition method that could form near-uniform nanostructured Pt-group overlayers on substrates has been reported, which involves redox replacement of an underpotential deposition (UPD) monolayer by more noble metal cations that could be reduced and simultaneously deposited.[17] Thus-tailored nanostructured films are of importance with regard to catalysis applications, due to their high surface-to-volume ratio. Weaver's group perfected the UPD-redox replacement technique to prepare Au nanoparticle film electrodes modified with uniform Pt-group overlayers and succeeded in surface-enhanced Raman scattering (SERs) applications.[18] Kwak et al. performed electrochemical measurements on various UPD systems on layered Au nanoparticle thin films.[19] Very recently, Adzic's group[20] in addition to us[21] have exploited the Pt submonolayers on metal nanoparticles such as Ru and Au nanoparticles as electrocatalysts. However, to the best of our knowledge, electrochemical modification of the

* To whom correspondence should be addressed. Fax: +86-431-5689711; e-mail: dongsj@ciac.jl.cn.

10.1021/jp051612e CCC: $30.25
Published on Web 07/27/2005

multi-deposited Pt overlayers on metal nanoparticle monolayer film electrodes has not yet been exploited for catalytic application to date.

In this paper, an alternately multiple UPD-redox replacement reaction technique was adopted to improve catalytic performance. A UPD Ag monolayer was first formed on the pre-modified Pt nanoparticle (PtNPs) monolayer films. Then, UPD Ag replacement with Pt (II) yielded a uniform Pt overlayer. When the modified electrode alternately undertook UPD-redox replacement reactions in a cyclic fashion, multiple-deposited Pt overlayer modified Pt nanoparticle (MD-Pt overlayer/PtNPs) monolayer films could be formed on a glassy carbon electrode (GCE) pretreated with 4-aminobenzoic acid (4-ABA). Such a tactic is plausible given that UPD Ag is known to form on Pt.[22] Interestingly, as compared to that of the pre-modified PtNPs monolayer films, thus-tailored nanostructured Pt films by multiple replacement cycles exhibit more positive potential and a higher current for dioxygen reduction and hydrogen evolution reactions (HER). The results provide clear evidence that the multi-deposited Pt overlayers with low loading could remarkably improve electrocatalytic activities, which aid in the design of catalysts for practical applications. Additionally, the film modified electrode also shows higher electrocatalytic activities than that of the bulk polycrystalline Pt electrode, in terms of both the reduction peak potential and the current density.

Experimental Procedures

Materials. 4-Aminobenzoic acid (4-ABA), K_2PtCl_4, and poly (diallyldimethylammonium chloride) (PDDA) were purchased from Aldrich. The absolute ethanol was dried over 3 Å molecular sieves, and lithium perchlorate was dried at about 90 ×bcC in a vacuum oven before use. $H_2PtCl_6 \cdot 6H_2O$, Ag_2SO_4, H_2SO_4, and other chemicals were of analytical reagent grade and used as received. Water used for preparation of aqueous solution was purified using a Millipore-Q water purification system.

Synthesis of Citrate-Stabilized Pt Colloids. One milliliter of 1% H_2PtCl_6 aqueous solution was added into 100 mL of water and then heated to boiling. Aging of the H_2PtCl_6 solution was not necessary in this synthetic procedure. Then, 3 mL of 1% sodium citrate aqueous solution was added rapidly, and the mixture was kept at a boiling temperature for ca. 30 min. Transmission electron microscopy (TEM) was used to examine particle size distribution, and an average diameter of 6 nm of Pt colloids was confirmed.

Preparation Procedure of the MD-Pt Overlayer/PtNPs Films. A GCE was treated with 4-ABA according to the published procedures.[23] The 4-ABA/GCE surface with the COOH group was first placed in an aqueous solution containing 8.0 wt % PDDA, providing a stable, positively charged surface on which the negatively charged citrate-stabilized PtNPs can be bound electrostatically. Then, the PtNPs were immobilized onto the PDDA/4-ABA/GCE by immersion of the latter into the sols for more than 12 h. A UPD Ag monolayer was formed on the PtNPs monolayer films by cycling the potential between 0 and +0.7 V at a scan rate of 20 mV/s for several cycles in 0.1 M H_2SO_4 containing 1 mM Ag_2SO_4. After thoroughly rinsing with water and drying with a nitrogen stream, the modified electrode was transferred to a solution of 5 mM K_2PtCl_4 in deaerated 0.1 M $HClO_4$ for 30 min to ensure the complete redox replacement of UPD Ag, which results in a Pt overlayer on the pre-modified PtNPs monolayer films. The modified electrode was then thoroughly rinsed and scanned in 0.1 M H_2SO_4 at the range of −0.2 to 1.5 V for several cycles. When the resulting modified electrode alternately undertook further UPD Ag/Pt-metal redox replacement cycles, the thickness and amount of Pt overlayers of the as-prepared film electrodes were readily adjusted by choosing different numbers of redox replacement cycles of UPD Ag.

Electrochemical Measurements. Electrochemical experiments were performed with a CHI 660 electrochemical workstation in a conventional three-electrode electrochemical cell using GCE (3 mm diameter) as the working electrode, twisted platinum wire as the auxiliary electrode, and Ag/AgCl as a reference electrode in aqueous media or Ag/Ag^+ (0.01 M $AgNO_3$) in anhydrous ethanol solutions. The GCEs were polished with 1.0 and 0.3 μm α-Al_2O_3 powders successively and sonicated in water for about 3 min after each polishing step. Finally, the electrodes were sonicated in ethanol, washed with ethanol, and dried with a high purity nitrogen stream immediately before use. Solutions were deaerated for at least 20 min with a high purity nitrogen stream and kept under a pressure of this gas during the experiments.

An EG and PARC model 636 rotating ring-disk electrode system and an EG and PARC model 366 bipotentiostat were used for RDE and RRDE voltammetry experiments. A rotating GC disk-platinum ring electrode (5 mm diameter) was used as a working electrode. The collection efficiency (N) of the ring electrode obtained by reducing ferricyanide at a disk electrode was 0.23. Before the experiments, the bulk Pt electrode (4 mm diameter) was mechanically polished and scanned in 0.1 M H_2SO_4 at the range of −0.2 to 1.5 V until CV characteristics for a clean Pt electrode were obtained.

Instrumentation. Samples for TEM were prepared by placing a drop of solution onto a carbon-coated copper grid and examined using a JEOL 2010 transmission electron microscope operated at 200 kV. X-ray photoelectron spectroscopy (XPS) measurement was performed on an ESCALAB-MKII spectrometer (VG Co.) with AlK_ (X-ray radiation as the X-ray source for excitation and analyzer pass energy of 50 eV). Typically, the operating pressure in the analysis chamber was below 10^{-9} Torr. The resolution of the spectrometer was 0.2 eV. Atomic force microscopy (AFM) measurements were performed on the GCE with a SPI3800N microscope (Seiko Instruments, Inc.). The images were acquired in the tapping mode. Measurements were made with the Si cantilever in air at room temperature. The force constant of the cantilever was 0.1−0.6 N/m with a scan rate of 1−2 Hz.

Results and Discussion

Fabrication of the MD-Pt Overlayer/PtNPs Films. The deposition protocol employed here is based on a new metal deposition method recently reported.[17] It involved a redox replacement of a UPD metal monolayer by more noble metal cations (such as late transition metal cations Pt and Pd) that are reduced and simultaneously deposited. The spontaneous redox replacement process, yielding a late transition-metal overlayer, is driven by the difference at equilibrium potentials between the transition metal and the UPD metal redox couples. For the system employed, $PtCl_4^{2-}/Pt$, the standard potentials ($E°$) of the corresponding half-reaction are more positive than those for the Ag^+/Ag_{UPD} couple.[24] So, the spontaneous redox replacement of a previously prepared UPD Ag monolayer by Pt (II) cations can be used to form Pt metal deposits, consistent with the anticipated balanced Ag → Ag^+/Pt (II) → Pt electron charge flow.

Through the attachment of 4-ABA containing the COOH group to GCE, the 4-ABA modified GCE was successively

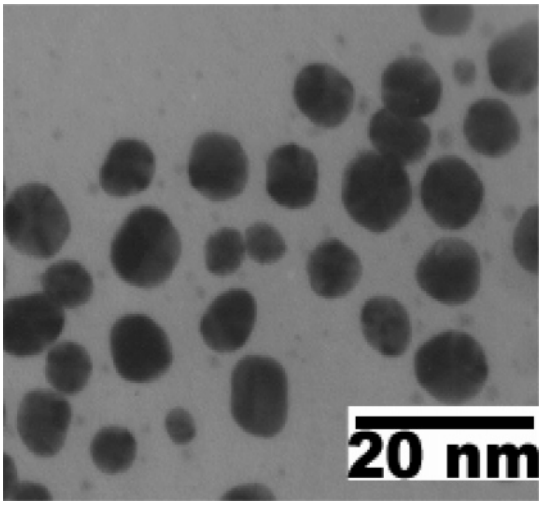

Figure 1. TEM image of PtNPs as templates for catalyst design (scale bar = 20 nm).

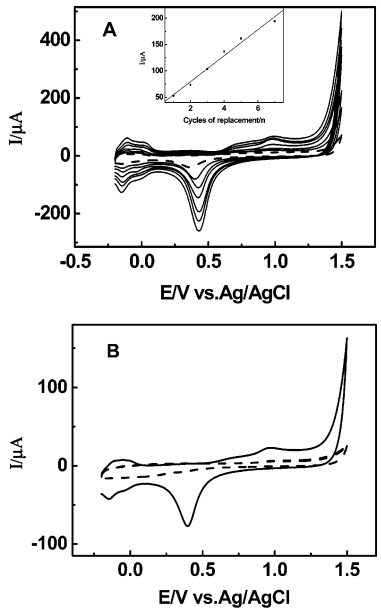

Figure 2. (A) CVs of the MD-Pt overlayer/PtNPs film electrodes with different redox replacement cycles of UPD Ag from K_2PtCl_4 solutions: $n = 1-5$ and 7 (from inside to outside), respectively. The dashed line represents the CV of the PtNPs monolayer film modified electrode. The inset shows a linear dependence of the platinum oxide reduction peak currents with the number of layers. (B) A comparison between the PtNPs films with one replacement cycle (solid line) and the control CV obtained on PDDA/4-ABA/GCE (PtNPs-free) after the same preparations (dashed line). Supporting electrolyte: 0.1 M H_2SO_4 solution and scan rate: 50 mV s^{-1}.

immersed in positively charged PDDA solutions and negatively charged citrate-stabilized PtNPs. Here, the aim of the effectively self-assembled PtNPs with relatively high loading as a template for the design of Pt overlayers catalyst was mainly to indicate that after replacement, the MD-Pt overlayers with very low loading could improve electrocatalytic activities remarkably. The average particle diameter of 6 nm was characterized by TEM as shown in Figure 1. Figure 2A (dashed line) shows a representative cyclic voltammogram (CV) obtained at the resulted PtNPs monolayer-modified electrode in 0.1 M H_2SO_4. The presence of the hydrogen adsorption/desorption peaks and preoxidation/reduction peaks shows familiar features of platinum electrochemistry.[25] The large current in the double-layer region

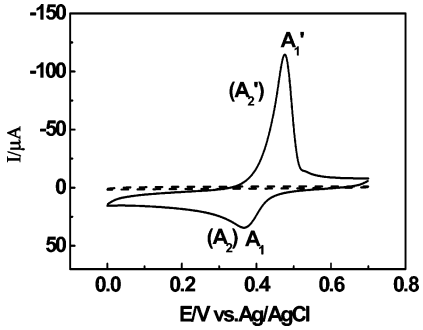

Figure 3. CV of PtNPs/PDDA/4-ABA/GCE in 0.1 M H_2SO_4 solution containing 1 mM Ag_2SO_4. The dashed line shows the control CV obtained on PDDA/4-ABA/GCE (PtNPs-free) after the same preparations. Scan rate: 20 mV s^{-1}.

is a familiar feature of large surface area material, which might reflect the nanoparticle nature of the electrode surface.[18,21]

Then, a solution of 1 mM Ag_2SO_4 and 0.1 M H_2SO_4 was used to deposit the Ag monolayer by the UPD method. Figure 3 displays CVs of UPD Ag on the PtNPs monolayer-modified electrode surface in a 1 mM Ag_2SO_4 + 0.1 M H_2SO_4 solution over a period of five successive scans. As seen in Figure 3, the feature is consistent with the formation of a UPD Ag monolayer.[26] On the negative-going sweep, one cathodic peak (A_1) is observed at ca. 0.369 V, corresponding to the formation of UPD Ag. One anodic peak at 0.476 V (A_1') is obtained on the positive-going sweep, consistent with the dissolution of UPD Ag. Thus, the modified electrode was then transferred to a deaerated solution containing 5 mM K_2PtCl_4 + 0.1 M $HClO_4$ at the open circuit for 30 min, resulting in a Pt overlayer on the pre-modified PtNPs monolayer films. It is noteworthy to mention that the Pt overlayer was selectively deposited on the PtNPs monolayer film, not on the GCE surface. In the control experiment, the PDDA/4-ABA/GCE after UPD Ag exhibits featureless responses of Ag as shown in Figure 3 (dashed line), indicating that the Ag monolayer cannot deposit on these sites without PtNPs.

The site-selective depositing of the Ag monolayer to PtNPs determines the selectivity of the Pt overlayer formed by redox replacement to particle sites, which can be reproducibly prepared by alternately undertaking further UPD Ag/Pt-metal redox replacement. With Pt as the redox-active species, the generation of the MD-Pt overlayers on particle surfaces results in reproducible electrochemical responses. Figure 2A shows representative CVs obtained from −0.2 to 1.5 V at the MD-Pt overlayer/PtNPs monolayer film electrode with different numbers of redox replacement cycles of UPD Ag from the K_2PtCl_4 solution. It can be seen that the CVs are similar to that of a polycrystalline Pt electrode,[25] displaying the characteristic anodic−cathodic current profile in which near-reversible peaks below 0 V are associated with hydrogen desorption−adsorption. Also, the irreversible feature corresponds to the formation and removal of a Pt surface oxide. In the control experiments (the Pt overlayers deposit in the absence of PtNPs), no distinctive Pt feature appears (dashed line in Figure 2B), validating that the Pt overlayers selectively deposited on PtNPs. Furthermore, we can see that when the first Pt overlayer is formed on the PtNPs monolayer films, the onset of the oxide formation and the peak potential of the oxide reduction are shifted more positively, indicating that the chemisorptions of OH on the Pt sites may be inhibited when the Pt overlayer is formed on the PtNPs films.[11] This may have a beneficial effect on the oxygen adsorption at a low overpotential and thus may lead to improvement in dioxygen reduction kinetics.[11,27] It also should

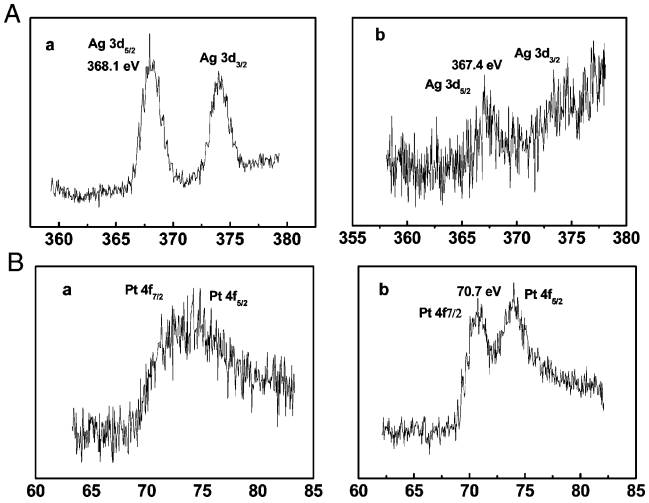

Figure 4. XPS spectra of PtNPs/PDDA/4-ABA/GCE show (A) Ag 3d: after UPD Ag (curve a) and Ag/Pt redox replacement (curve b) and (B) Pt 4f: before (curve a) and after one Pt overlayer deposition by one replacement cycle (curve b).

be mentioned here that no observable changes in the shape and height of the CVs are found during the whole electrochemical measurements and that the real surface area of the Pt catalyst keeps an almost constant value even when there is continuous cycling between −0.2 and 1.5 V, which excludes the possibility of severe agglomeration and sintering and also indicates that the catalyst is very stable. In addition, with increasing the number of redox replacement cycles, the redox peak currents increase gradually. Taking the platinum oxide reduction peak as an example, a good linear relationship between the cycles and the cathodic peak currents of the Pt overlayers (the inset of Figure 2A) demonstrates that equal amounts of Pt overlayers are deposited in each UPD-replacement cycle and also that the film grows uniformly.

XPS Measurement. XPS measurements were also performed to identify and characterize the as-prepared PtNPs film as shown in Figure 4. The XPS spectrum of the Ag $3d_{3/2}$ and Ag $3d_{5/2}$ doublet in the zero oxidation state before a redox replacement reaction demonstrates the successful UPD Ag on the PtNPs monolayer films (curve a in Figure 4A). After a redox replacement reaction with K_2PtCl_4, there is little residual silver left as shown in curve b of Figure 4A. It is possible that a bimetallic interaction or possible alloying between silver and platinum cannot be totally excluded. In addition, as shown in CV of UPD Ag (Figure 3), the broadness and asymmetry of the peak may also reflect the process of the Ag−Pt surface alloying to a certain extent, probably arising from the influence of the grain defect feature (such as steps, kinks, and edges) of the nanofilms on the electrochemical behaviors and also from the overlap of another couple of peaks (labeled A_2 and A_2').[26] Also, citrate-stabilized PtNPs before the redox replacement reaction were not in the completely zero state as shown in curve a of Figure 4B. After a replacement reaction, the Pt $4f_{7/2}$ and Pt $4f_{5/2}$ doublet in the zero oxidation state appear, indicating the complete formation of Pt (0) (curve b in Figure 4B).

AFM Measurement. The surface morphology of the films was examined by AFM. Figure 5A,B presents the morphological image of the PtNPs monolayer films and the MD-Pt overlayer/PtNPs films by three replacement cycles, respectively. Lateral dimensions are distorted due to the convolution with the AFM tip. The cross-sectional contour plots of surface morphology give a particle height of ca. 6−15 nm for the immobilized PtNPs and 8−16 nm for the MD-Pt overlayers by three replacement

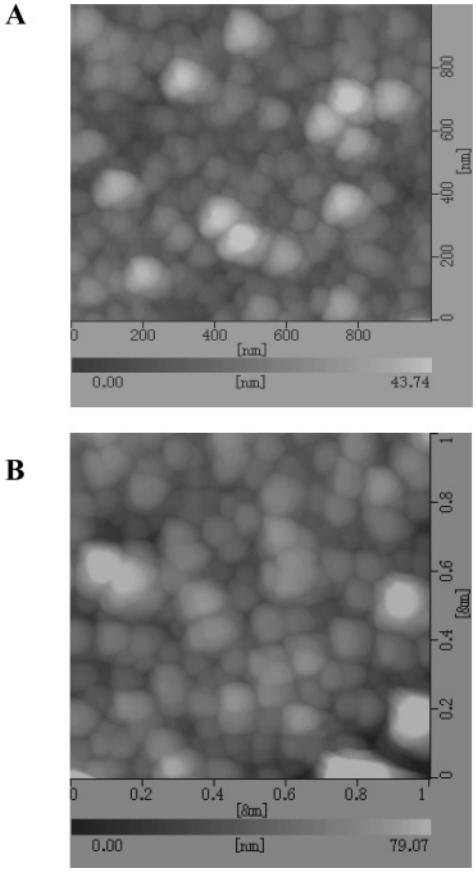

Figure 5. AFM images of the only PtNPs monolayer films (A) and the MD-Pt overlayer/PtNPs films by three replacement cycles (B).

cycle modified PtNPs. Although there are some agglomerated blocks also existing in the films, it can be clearly seen that after multiple replacement cycles, the diameter of the PtNPs has no remarkable change as compared to that of the PtNPs before replacement. In addition, the surface roughness of the film increases from 8.2 to 14.4 nm after replacement cycles.

Electrocatalytic Reduction of Dioxygen on the MD-Pt Overlayer/PtNPs Films. Our interest in the MD-Pt overlayer/PtNPs films is primarily related to electrocatalytic applications. The electrocatalytic activity of the system employed here for dioxygen reduction was investigated in detail. Figure 6A presents CVs of the MD-Pt overlayer/PtNPs film electrodes with different numbers of replacement cycles in a 0.1 M H_2SO_4 solution in the presence and absence of dioxygen. The dotted line corresponds to CV of the MD-Pt overlayer/PtNPs films formed by seven redox replacement cycles of UPD Ag from K_2PtCl_4 in a N_2-saturated 0.1 M H_2SO_4 solution. In the presence of dioxygen, a remarkable catalytic reduction peak current occurs at 0.57 V, which shifts ca. 210 mV more positive than that of a typical Pt catalyst in 0.5 M H_2SO_4.[28] In addition, the reduction potential obtained is more positive than those recently reported by our group[14,29] and another group[13] for PtNPs in the multilayered film modified GCE in 0.5 M H_2SO_4 and also Martin's group[30] for PtNPs-containing carbon nanotubule membranes. Here, it is noted that with the increase of the H_2SO_4 concentration, the reduction potential shifts more positively. Interestingly, when the first Pt overlayer is formed on the PtNPs films by the UPD-redox replacement technique, its peak potential for dioxygen reduction shifts positively in comparison to that of the PtNPs monolayer films (dashed line in Figure 6A), which indicates that the electrocatalytic activity of the films is enhanced with the Pt overlayers forming on the PtNPs

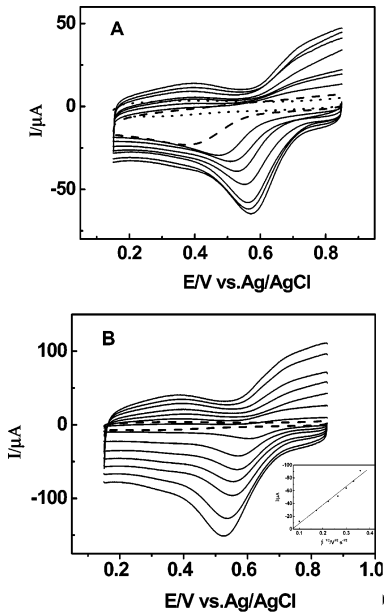

Figure 6. (A) CVs of O_2 reduction at the MD-Pt overlayer/PtNPs film electrodes with different redox replacement cycles: $n = 1-4$, 6, and 7 (from top to bottom), respectively. The dotted line is the CV at the MD-Pt overlayer/PtNPs films by seven replacement cycles in N_2-saturated 0.1 M H_2SO_4 solution. The dashed line is the CV of O_2 reduction at the PtNPs monolayer film electrodes. Supporting electrolyte: air-saturated 0.1 M H_2SO_4 solution and scan rate: 50 mV s^{-1}. (B) CVs of O_2 reduction at the MD-Pt overlayer/PtNPs film electrodes by seven replacement cycles with different scan rates: 0.01, 0.03, 0.05, 0.07, 0.09, 0.11, and 0.13 V s^{-1}. The dashed line is the CV at 0.01 V s^{-1} in N_2-saturated 0.1 M H_2SO_4 solution. The inset shows a linear dependence of the electrocatalytic dioxygen reduction peak currents with the square root of scan rates. Supporting electrolyte: air-saturated 0.1 M H_2SO_4 solution.

surfaces. It also can be seen that with increasing the number of replacement cycles, the catalytic current of dioxygen reduction increases gradually, and interestingly, the reduction peak potential shifts positively. Therefore, by simply choosing different numbers of replacement cycles, the amount of Pt overlayers of the as-prepared films was readily adjusted while enhancing the catalytic activity toward dioxygen reduction. It is possible that a lack of a significant inhibition of the PtOH might be partly responsible for the enhanced dioxygen reduction kinetics.[20,31] In addition, by the multiple UPD-replacement technique, the surface structure of the PtNPs might be changed (such as low coordination of a considerable number of surface atoms and an enhanced surface roughness),[31] as compared to that of the PtNPs monolayer films, thus decreasing the activation energy of the dioxygen reduction reaction. Therefore, the reduction peak potential shifts positively. The results provide clear evidence that after multiple replacement cycles, the multi-deposited Pt overlayers with very low loading can remarkably improve the electrocatalytic activities.

Figure 6B shows CVs of dioxygen reduction at the as-prepared film electrodes in an air-saturated 0.1 M H_2SO_4 solution at different scan rates. The peak currents of dioxygen reduction vary as a linear function of the square root of the scan rates, demonstrating that the kinetics of the overall process is controlled by mass transport of dioxygen from the bulk solution to the modified electrode surface.

For the purpose of comparison, voltammograms for O_2 reduction at a bulk polycrystalline Pt electrode and the MD-Pt overlayer/PtNPs film electrodes prepared by one and seven replacement cycles are shown in Figure 7. Compared with that of the bulk Pt electrode (curve a), the as-prepared modified

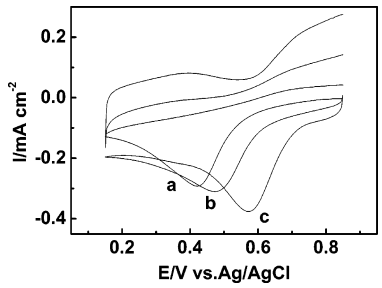

Figure 7. CVs for O_2 reduction at the bulk Pt electrode (curve a) and the MD-Pt overlayer/PtNPs film electrodes by one (curve b) and seven (curve c) replacement cycles. Supporting electrolyte: air-saturated 0.1 M H_2SO_4 solution and scan rate: 50 mV s^{-1}.

electrode by one redox replacement (curve b) exhibits more positive potential for dioxygen reduction. Increasing the number of replacement cycles to seven times (curve c), the catalytic activity is enhanced obviously, in terms of both reduction peak potential and current density. From curve c, the reduction peak potential is comparable with that of the most positive achievable by currently available catalysts in solutions containing 1 M H^+ (0.55 V vs the SCE),[32] and the current density is slightly higher than that of the bulk Pt electrode, which saves precious metal Pt.

Kinetic Analysis of Dioxygen Reduction on the MD-Pt Overlayer/PtNPs Films. To study the kinetics of the catalytic reduction of dioxygen, voltammetric measurements at RDE and RRDE have been performed. Figure 8A reveals current−potential curves of dioxygen reduction in air-saturated 0.1 M H_2SO_4 at various rotation rates using the rotating glassy carbon (GC) disk electrode assembled with the MD-Pt overlayer/PtNPs films by seven replacement cycles. It can be seen that potential-independent plateau currents are present at all rotation rates and that the catalytic current increases gradually with the increase of the electrode rotation rate. The Levich and Koutecky−Levich plots obtained from the plateau currents at 0.30 V (Figure 8A) are shown in Figure 8B,C, respectively. If the mass-transport process in the solution solely controls the reduction of dioxygen at the MD-Pt overlayer/PtNPs film electrodes, the relationship between limiting current and rotation rate should obey the Levich equation.[33] From Figure 8B, the limiting current increases linearly with the square root of the rotation rate at lower rotation rates and then deviates slightly from the Levich plot, which has been observed in other systems.[34] This suggests that the catalytic reaction is controlled not by diffusion but by kinetics. The slope of the Levich plot is very close to that of the calculated line for the four-electron reduction of O_2. When the mass-transport process in the solution and the catalytic reaction becomes dominant, the Koutecky−Levich equation[33] can be used to determine the number of electrons transferred for the O_2 reduction and the rate constant for the catalytic reaction rate between film electrodes and O_2. As seen from Figure 8C, the Koutecky−Levich plot is linear with a slope very close to that of the dashed line calculated for the four-electron reduction of O_2 by a kinetics-controlled process. The calculated number of electrons involved in the reduction of O_2 from the slope of the Koutecky−Levich plot is found to be about 3.80 for the MD-Pt overlayer/PtNPs films.[33] The kinetic current value obtained from the intercept of the Koutecky−Levich plot is founded to be 17.3 mA. The rate constant, calculated from the kinetic current value, is found to be 0.40 cm s^{-1}, which is higher than that reported for Pt (110), the most active face at almost the same potential.[35] Such a large rate may be attributed to the decrease in the coverage of PtOH, which can enhance O_2 reduction kinetics.[36]

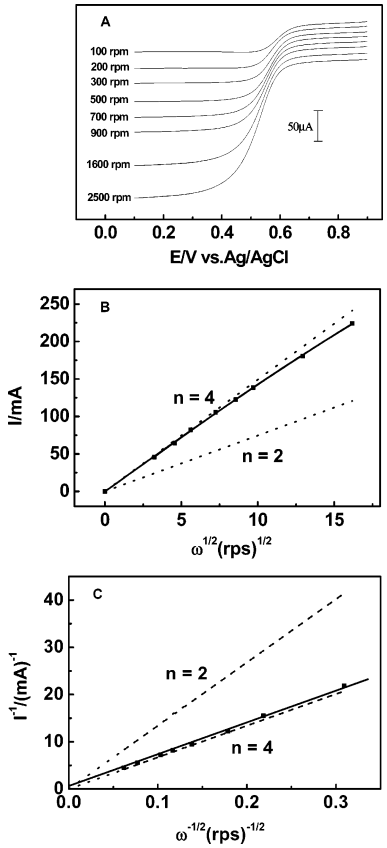

Figure 8. (A) Current−potential curves of O_2 reduction at a RDE assembled with the MD-Pt overlayer/PtNPs films by seven replacement cycles with different rotating rates in air-saturated 0.1 M H_2SO_4 solution. Levich plot (B) and Koutecky−Levich plot (C) of the kinetic limiting currents of the voltammograms. The solid line is from the experimental data, and the dashed lines are from the calculated data considering the reduction of O_2 by two and four electrons, respectively.

The Tafel behavior in the mixed kinetic-diffusion controlled region was also investigated using mass transport-corrected Tafel plots of E versus log $[i/(i_l - i)]$ for the MD-Pt overlayer/PtNPs film electrodes by seven replacement cycles at a rotation rate of 2500 rpm (figure not shown). It is well-known that the bulk polycrystalline Pt shows two Tafel slope regions, in which the small Tafel slope of ca. −60 mV/decade (the low potential region) corresponds to O_2 electroreduction at the oxidized (PtOH) surface, whereas the large Tafel slope of ca. −120 mV/decade (the high potential region) corresponds to that at a clean Pt surface.[37,38] The transition in the two Tafel slopes is probably related to the potential-dependent coverage of surface oxides like PtOH, which inhibit the adsorption of O_2.[31,39] For the MD-Pt overlayer/PtNPs film electrodes, the result shows that the transition in the Tafel slopes at the entire potential region is absent. The single Tafel slope −113 mV/decade was obtained, suggesting that there was a lack of a significant inhibition of PtOH on the Pt overlayers,[20,39] which is in agreement with the results obtained from the growth process of the MD-Pt overlayers characterized by cyclic voltammetry. It is close to the value of −120 mV/decade, indicating that the transfer of the first electron to O_2 was the rate-limiting step in four-electron reduction of dioxygen.

A rotating GC disk−platinum ring electrode was employed to determine the quantity of H_2O_2 that was generated by a two-electron reduction process of O_2 at the disk electrode, which will give direct evidence to detect the effectiveness of this catalyst through four-electron reduction of dioxygen to water. Figure 9 shows the voltammetric curves for the reduction of dioxygen, recorded at RRDE with the MD-Pt overlayer/PtNPs films by seven replacement cycles immobilized on the GC disk electrode. The disk potential was scanned from 0.9 to 0.1 V, while the ring potential was held at 1.0 V to oxidize H_2O_2 generated by O_2 reduction at the disk electrode. Only a very small ring current was observed as the potential was swept through the electrocatalytic reduction potential, which indicated almost no H_2O_2 production by the catalyst. The ratio of the ring to the disk current, i_R/i_D, is 0.002 for the MD-Pt overlayer/PtNPs films, which is much smaller than the collection efficiency of 0.20 (standard deviation 0.02) determined with the use of the $[Fe(CN)_6]^{3-/4-}$ redox couple under the same solution conditions. From the value of i_R/i_D, 0.002, the calculated number of electrons involved in the reduction of O_2 was found to be 3.98 according to the equation $n = 4 - 2(i_R/i_D N)$,[40] which is almost identical to that acquired from the Koutecky−Levich plot (vide supra). Also, from the value of i_R/i_D, 0.002, the efficiency of H_2O formation of the MD-Pt overlayer/PtNPs films amounts to 98 ± 0.2%.[41] This result indicates that the reduction of dioxygen at the MD-Pt overlayer/PtNPs film electrodes mainly supports the four-electron pathway process, realizing nearly complete electroreduction for dioxygen to water.

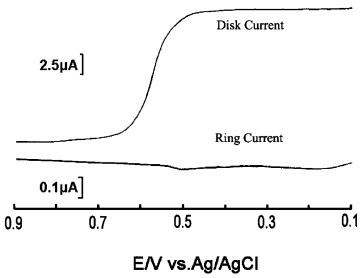

Figure 9. RRDE voltammograms of the MD-Pt overlayer/PtNPs film electrodes by seven replacement cycles (disk scan rate: 20 mV s^{-1} and ω: 100 rpm) in air-saturated 0.1 M H_2SO_4 solution. The potential of the platinum ring electrode was set to 1.0 V to oxidize H_2O_2 to O_2 completely.

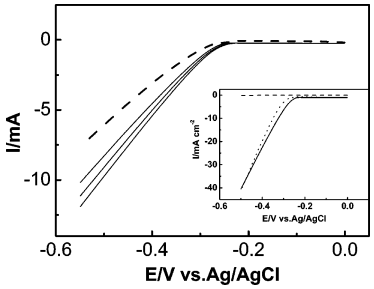

Figure 10. Polarization curves for the HER on the MD-Pt overlayer/PtNPs films with different redox replacement cycles of 1, 3, and 7. The dashed line is the polarization curve on the only PtNPs monolayer films. The inset represents polarization curves for the HER on the bare GCE (dashed line), bulk Pt electrode (dotted line), and the MD-Pt overlayer/PtNPs films by seven replacement cycles (solid line). Supporting electrolyte: N_2-saturated 0.1 M H_2SO_4 solution, scan rate: 5 mV s^{-1}, and rotation rate: 3500 rpm.

Electrocatalytic Activities for HER of the MD-Pt Overlayer/PtNPs Films. The electrocatalytic activity of thus-prepared modified electrode for HER was also investigated. Figure 10 shows polarization curves for the HER on the MD-Pt overlayer/PtNPs films with different numbers of replacement cycles in N_2-saturated 0.1 M H_2SO_4 solutions. The dashed line represents the polarization curve on the only PtNPs film without a UPD-replacement reaction. With the increase of the replacement steps, the current for the HER increases gradually. We

also evaluated the electrocatalytic ability of the MD-Pt overlayer/PtNPs films with respect to the HER in a 0.1 M H_2SO_4 solution as compared with a bulk Pt electrode and bare GCE (the inset of Figure 10). As seen from the inset, the current density value of the HER at the MD-Pt overlayer/PtNPs films by seven replacement cycles is slightly higher than that obtained at the bulk Pt electrode, and the hydrogen evolution potential is more positive than that of the latter. Importantly, the current at the MD-Pt overlayer/PtNPs films does not decay as quickly as that at the bulk polycrystalline Pt electrode. There is no observable decrease in the current density at the MD-Pt overlayer/PtNPs films after 1 h, whereas it is known that activated Pt electrodes lose most of their electrocatalytic activity during a period of ca. 1 h (up to 90% in acid solutions).[42] Even overnight, the current density at the MD-Pt overlayer/PtNPs films only decreased 5%. So, the as-prepared modified electrode is very durable and efficient in longer time periods.

In addition, in comparison to that of bulk Pt electrodes, the CVs of PtNPs monolayer film electrodes and the MD-Pt overlayer/PtNPs film modified electrode show some distortion of the hydrogen adsorption and desorption peaks (figure not shown), which may imply a difference in H adsorption behavior between modified electrode and bulk Pt electrode.[43] Also, shifts in the peak potential of H adsorption can be observed in the CVs of PtNPs monolayer films electrode and the MD-Pt overlayers/PtNPs film modified electrode, which indicates that changes may be made in the binding energy of adsorbed hydrogen, caused by some change in the electronic nature of the MD-Pt overlayers/PtNPs film electrode.[43] However, now it is difficult to determine precisely the main factor effecting chemical properties of the film modified electrode, since the details about it are probably very complicated and need to be studied using other techniques. Further investigation into the details is underway.

Stability of the MD-Pt Overlayer/PtNPs Films. The stability of the MD-Pt overlayer/PtNPs film electrodes by comparing the changes in voltammetric peak currents before and after potential scanning 4 h between −0.2 and 1.5 V at 50 mV s^{-1} in 0.1 M H_2SO_4 was found. There was no remarkable change in the voltammetric currents of Pt and the catalytic current. Furthermore, no observable change in the shape and height of the catalytic current was found, after the as-prepared modified electrode was exposed to air or soaked in the supporting electrolyte for 2 months. Chronoamperometry experiments show that the MD-Pt overlayer/PtNPs film exhibits a better stability and is able to maintain higher current density for over 1 h, as compared to that of the bulk Pt electrode. The MD-Pt overlayer/PtNPs films are very stable and difficult to remove from the electrode surface. The only way to remove the film is to polish the electrode. The good stability of the films is very useful in the preparation of the modified electrode and the catalytic reaction.

Conclusion

Overall, the present results demonstrate an electrochemical strategy to nanoparticle-based catalyst design using the multiple UPD-redox replacement technique. The preparation method is very simple, controllable, and reproducible, and the as-prepared film electrodes have a high mechanical stability and are very robust, durable, and efficient in long time periods. RDE voltammetry and RRDE voltammetry demonstrate that the MD-Pt overlayer/PtNPs films can catalyze almost four-electron reduction of O_2 to H_2O in air-saturated 0.1 M H_2SO_4. Thus-prepared nanostructured Pt films exhibit relatively high electrocatalytic activities for dioxygen reduction, in terms of both reduction peak potential and current density, when compared to that of the bulk polycrystalline Pt electrode. Interestingly, after multiple replacement cycles, the electrocatalytic activities were improved remarkably, although the increased amount of Pt is very low in comparison to that of pre-modified PtNPs due to the intrinsic feature of a UPD-redox replacement technique. The results indicate that the multiple replacement cycles are beneficial for the improvement of the catalytic performance. In a word, through using the technique of tailoring the catalytic surface, the electrocatalytic activities could be improved without using very much Pt. These features may provide an interesting way to produce Pt catalysts with reliable catalytic performance and a reduction of costs. Additionally, this approach could be extended to the fabrication of nanostructured Au and Pd deposits and will be attractive to the design of nanoparticle-based materials for catalytic applications.

Acknowledgment. This work was supported by the National Natural Science Foundation of China (20275036 and 20210506).

References and Notes

(1) Hamman, C. H.; Hamnett, A.; Vielstich, W. *Electrochemistry*; Wiley-VCH: New York, 1998; Ch. 9.

(2) Bockris, J. O. M.; Reddy, A. K. N. *Modern Electrochemistry*; Kluwer Academic/Plenum: New York, 2000; Vol. 2B, p 1191.

(3) Adzic, R. R. *Recent Advances in the Kinetics of Oxygen Reduction.* In *Electrocatalysis*; Lipkowski, J.; Ross, P. N., Eds.; Wiley-VCH: New York, 1998; pp 197−242.

(4) Marković, N. M.; Schmidt, T. J.; Stamenkoviæ, V.; Ross, P. N. *Fuel Cells* **2001**, *1*, 105.

(5) Matsumoto, E.; Uesugi, S.; Koura, N.; Okajima, T.; Ohsaka, T. *J. Electroanal. Chem.* **2001**, *505*, 150.

(6) Song, E.; Shi, C.; Anson, F. C. *Langmuir* **1998**, *14*, 4315.

(7) Liang, H. P.; Zhang, H. M.; Hu, J. S.; Guo, Y. G.; Wan, L. J.; Bai, C. L. *Angew. Chem., Int. Ed.* **2004**, *43*, 1540.

(8) Filhol, J. S.; Simon, D.; Sautet, P. *J. Am. Chem. Soc.* **2004**, *126*, 3228.

(9) Huang, M. H.; Bi, L. H.; Shen, Y.; Dong, S. J. *J. Phys. Chem. B* **2004**, *108*, 9780.

(10) Yan, T.; Niwa, O.; Horiuchi, T.; Tomita, M.; Iwasaki, Y.; Ueno, Y.; Hirono, S. *Chem. Mater.* **2002**, *14*, 4796.

(11) Yang, H.; Alonso-Vante, N.; Léger, J.-M.; Lamy, C. *J. Phys. Chem. B* **2004**, *108*, 1938.

(12) Salgado, J. R. C.; Antolini, E.; Gonzalez, E. R. *J. Phys. Chem. B* **2004**, *108*, 17767.

(13) Kulesza, P. J.; Chojak, M.; Karnicka, K.; Miecznikowski, K.; Palys, B.; Lewera, A. *Chem. Mater.* **2004**, *16*, 4128.

(14) Huang, M. H.; Shao, Y.; Sun, X. P.; Chen, H. J.; Liu, B. F.; Dong, S. J. *Langmuir* **2005**, *21*, 323.

(15) Choi, K.-S.; McFarland, E. W.; Stucky, G. D. *Adv. Mater.* **2003**, *15*, 2018.

(16) Somorjai, A. G. *Introduction to surface chemistry and catalysis*; Wiley: New York, 1994.

(17) Brankovic, S. R.; Wang, J. X.; Adziæ, R. R. *Surf. Sci.* **2001**, *474*, L173.

(18) Park, S.; Yang, P. X.; Corredor, P.; Weaver, M. J. *J. Am. Chem. Soc.* **2002**, *124*, 2428.

(19) Lee, J.; Hwang, S.; Lee, H.; Kwak, J. *J. Phys. Chem. B* **2004**, *108*, 5372.

(20) Sasaki, K.; Mo, Y.; Wang, J. X.; Balasubramanian, U. F.; McBreen, J.; Adzic, R. R. *Electrochim. Acta.* **2003**, *48*, 3841.

(21) Jin, Y. D.; Shen, Y.; Dong, S. J. *J. Phys. Chem. B* **2004**, *108*, 8142.

(22) Rodriguez, J. F.; Taylor, D. L.; Abruña, H. D. *Electrochim. Acta* **1993**, *38*, 235.

(23) Liu, J. Y.; Cheng, L.; Liu, B. F.; Dong, S. J. *Langmuir* **2000**, *16*, 7471.

(24) Crooks, R. M.; Zhao, M.; Sun, L.; Chechik, V.; Yeung, L. K. *Acc. Chem. Res.* **2001**, *34*, 181.

(25) For example: Conway, B. E. *Prog. Surf. Sci.* **1995**, *49*, 331.

(26) Jin, Y. D.; Dong, S. J. *J. Phys. Chem. B* **2003**, *107*, 13969.

(27) Paulus, U. A.; Wokaun, A.; Scherer, G. G.; Schmidt, T. J.; Stamcnkovic, V.; Markovic, N. M.; Ross, P. N. *Electrochim. Acta* **2002**, *48*, 263.

(28) Perez, J.; Gonzalez, E. R.; Ticianelli, E. A. *J. Electrochem. Soc*. **1998**, *145*, 2307.
(29) Shen, Y.; Liu, J. Y.; Wu, A. G.; Jiang, J. G.; Bi, L. H.; Liu, B. F.; Li, Z.; Dong, S. J. *Langmuir* **2003**, *19*, 5397.
(30) Che, G. L.; Lakshmi, B. B.; Fisher, E. R.; Martin, C. R. *Nature* **1998**, *393*, 346.
(31) Zhang, J.; Mo, Y.; Vukmirovic, M. B.; Klie, R.; Sasaki, K.; Adzic, R. R. *J. Phys. Chem. B* **2004**, *108*, 10955.
(32) Anson, F. C.; Shi, C.; Steiger, B. *Acc. Chem. Res.* **1997**, *30*, 437.
(33) Bard, A. J.; Faulkner, L. R. *Electrochemical Methods, Fundamentals, and Applications*; Wiley: New York, 1980; Ch. 8, p 288.
(34) Souza, F. D.; Hsieh, Y. Y.; Deviprasad, G. R. *Chem. Commun*. **1998**, 1027.
(35) Perez, J.; Villullas, H. M.; Gonzalez, E. R. *J. Electroanal. Chem*. **1997**, *435*, 179.
(36) Chen, S. L.; Kucernak, A. *J. Phys. Chem. B* **2004**, *108*, 3262.
(37) Mano, N.; Fernandez, J. L.; Kim, Y.; Shin, W.; Bard, A. J.; Heller, A. *J. Am. Chem. Soc*. **2003**, *125*, 15290.
(38) Toda, T.; Igarashi, H.; Uchida, H.; Watanabe, M. *J. Electrochem. Soc*. **1999**, *146*, 3750.
(39) Markoviæ, N. M.; Gasteiger, H. A.; Ross, P. N. *J. Phys. Chem.* **1995**, *99*, 3411.
(40) Liu, S.; Xu, J.; Ran, H.; Li, D. *Inorg. Chim. Acta* **2000**, *306*, 87.
(41) Jakobs, R. C. M.; Janssen, L. J. J.; Barendrecht, E. *Electrochim. Acta* **1985**, *30*, 1085.
(42) Conway, B. E.; Bai, L. J. *J. Electroanal. Chem.* **1986**, *198*, 149.
(43) Hutton, H. D.; Pocard, N. L.; Alsmeyer, D. C.; Schueller, O. J. A.; Spontak, R. J.; Huston, M. E.; Huang, W. H.; McCreery, R. L.; Neenan, T. X.; Callstrom, M. R. *Chem. Mater.* **1993**, *5*, 1727.